# BVRI Photometric Observations, Light Curve Solutions and Orbital Period Analysis of BF Pav

**Atila Poro[1], Mark G. Blackford[2], Fatemeh Davoudi[1], PegahSadat MirshafieKhozani[1], Fahri Alicavus[3,4], Jabar Rahimi[1], Behjat Zarei Jalalabadi[1], Farzaneh Ahangarani Farahani[1], Edwin Budding[5]**

[1]The International Occultation Timing Association Middle East section, Iran, info@iota-me.com
[2]Variable Stars South (VSS), Congarinni Observatory, Congarinni, NSW, Australia 2447, Australia
[3]Çanakkale Onsekiz Mart University, Faculty of Arts and Sciences, Department of Physics, 17020, Çanakkale, Turkey
[4]Çanakkale Onsekiz Mart University, Astrophysics Research Center and Ulupınar Observatory, 17020, Çanakkale, Turkey
[5]Carter Observatory, 40 Salamanca Rd, Kelburn, Wellington 6012, New Zealand

## Abstract

The new ephemeris and light curve analysis by synthesizing our mid-eclipse times and the former observations of BF Pav, that is classified as a W UMa-type eclipsing binary, are presented in this study. We also obtain this binary system's period changes using Wilson-Devinney code after five nights of observation utilizing BVRI filters. Our results demonstrate that BF Pav is a contact binary system with a photometric mass ratio $q = 0.94$, and a fillout factor $f = 13\%$. We also calculated the distance of BF Pav $d = 250 \pm 27$ pc from distance modulus formula, which is in good agreement with the distance obtained from this binary system's parallax in Gaia DR2. From our O-C analysis, we found a continuous period increase at a rate of 0.3086634× $10^{-7}$ $day/yr$ which corresponds to a period increase of 0.266 s $century^{-1}$. We determined the mass of each component of this binary system using two different methods and compare our results with the former study's results.

## Keywords

Techniques: photometric; Stars: binaries: eclipsing; Stars: individual: BF Pav

## Introduction

W UMa-type binary systems have short orbital periods less than a day showing continuous light variations (Dryomova and Svechnikov, 2006). They include two stars usually surrounded by a common envelope resulting from mass overflowing one star's Roche lobe (Smith, 1984).
The BF Pav binary system, which is located in the constellation of Pavonis in the Southern Hemisphere Sky, is a variable star of W UMa-type with an approximate period of 0.302318 days and G8 Spectral type (Gonzalez et al., 1996). Its apparent magnitude in V filter is 12.17 (APASS9). The variability of BF Pav was discovered by Shapley in 1939 (Gonzalez et al., 1996) and the first photoelectric light curve was obtained by Hoffman (1981). Although these observations did not cover the complete orbital period, the observer derived a period of 0.3056 days. Between 1987 and 1993, BF Pav was observed photoelectrically in the UBV filters in the observational program of Southern Short-Period Eclipsing Binaries to determine the time of minima, photometric and absolute parameters. The photometric solution adopted a mass ratio of q = 1.4 ± 0.2, a fillout factor equals to 10%, and efficient thermal contact between the components, ΔT≃100 K (Gonzalez et al., 1996).
Dryomova and Svechnikov (2006) found the rate of change of the period of BF Pav to be $\dot{p}$ = 1.62×10-7 day/yr in their study of variation in the orbital period of W Uma-type contact systems. Zhang et al. (2015) noted that BF Pav has a similar period increase to GK Aqr.
In this paper, we present a new ephemeris based on our observations as well as new period change analysis and light curve solutions.

## Observation and data reduction

The observation of the BF Pav was carried out in August 2019 and July 2020 during five individual nights and a total of 2054 images were taken with a 14" Ritchey Chretien telescope and SBIG STT3200-ME CCD (2148x1510 pixels each 6.8-micron square) equipped with Astroden Johnson-Cousins BVRI Filters at the Congarinni Observatory which is located in Australia with geographical coordinates 152° 52´ East and 30° 44´ South and 20 meters above the mean sea level. Each frame was recorded at 2×2 binning with 50 seconds exposure time in each filter and CCD temperature set at -15°C.

GSC 8770-1511 was chosen as a check star and 8 stars were chosen as comparison stars with appropriate apparent magnitude in comparison to BF Pav. The general characteristics of BF Pav with the comparisons and the check star are shown in Table 1 and Figure 1 shows an observed field-of-view of these stars.

**Table 1. Characteristic of the Variable star, the Check star, and the Comparison stars (from: SIMBAD[1] and Vizier-APASS9[2]).**

| Star type | Star name | RA. (2000) | DEC. (2000) | Magnitude (V) |
|---|---|---|---|---|
| Variable | BF Pav | 18 45 39.32 | -59 38 25.87 | 12.17 |
| Comparison1 | GSC 8770-1107 | 18 45 30.01 | -59 32 34.9 | 12.23 |
| Comparison2 | GSC 8770-1582 | 18 45 50.08 | -59 36 59.1 | 13.43 |
| Comparison3 | GSC 8770-1663 | 18 45 49.66 | -59 37 48.9 | 13.43 |
| Comparison4 | GSC 8770-0085 | 18 45 33.39 | -59 39 50.5 | 13.52 |
| Comparison5 | GSC 8770-103 | 18 46 0.36 | -59 36 5.8 | 12.18 |
| Comparison6 | GSC 8770-1383 | 18 45 42.38 | -59 32 5.3 | 13.39 |
| Comparison7 | GSC 8770-1325 | 18 45 18.25 | -59 44 27.2 | 13.23 |
| Comparison8 | GSC 8770-1333 | 18 45 56.89 | -59 40 26.6 | 13.54 |
| Check | GSC 8770-1511 | 18 45 32.73 | -59 36 25.0 | 13.48 |

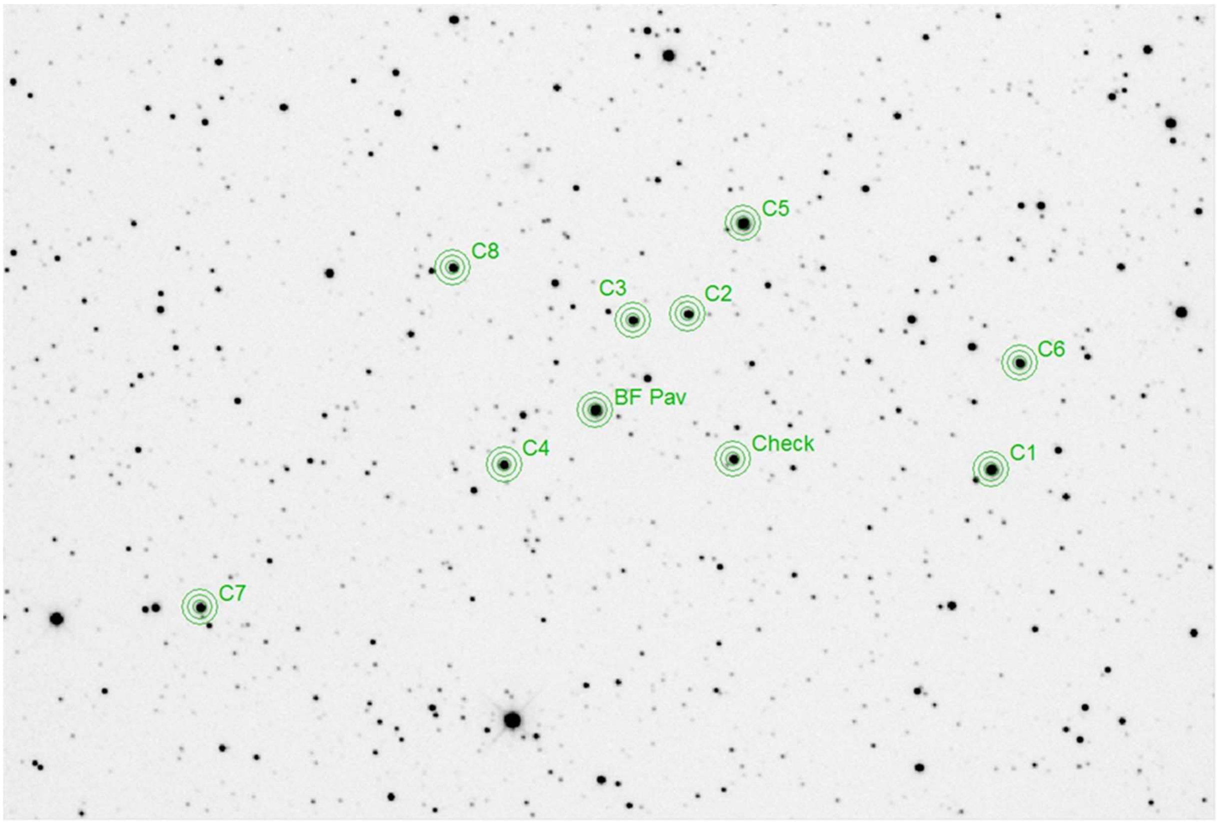


**Figure 1. Observed field-of-view for BF Pav, comparison stars (C1 – C8), and a check star.**

[1]http://simbad.u-strasbg.fr/simbad/
[2]http://vizier.u-strasbg.fr/viz-bin/

Standard procedures for CCD image processing (aligned pictures, bias and dark removal, flat-fielding to correct for vignetting, and pixel-to-pixel variations) are applied. We did all picture processing and plotting raw images with MaxIm DL software. Then more modifications were made with AstroImageJ (AIJ) software (Collins et al., 2017). AIJ is a powerful tool for astronomical image analysis and precise photometry (Davoudi et al., 2020).
We determined eight primary and seven secondary minimum times from the observed light curves in BVRI filters. These minima were calculated by using the Kwee and van Woerden (1956) method and they are listed in Table 2. The observed and synthetic light curves in BVRI filters with residuals show in Figure 2.

**Table 3. Times of minima in different filters of BF Pav.**

| Filter | Min. 1 ($BJD_{TDB}$) | Min. 2 ($BJD_{TDB}$) |
|---|---|---|
| I | 2458713.9377 ± 0.0001 | 2458714.0882 ± 0.0001 |
| B | 2458713.9380 ± 0.0002 | 2458714.0883 ± 0.0002 |
| V | 2458713.9377 ± 0.0001 | 2458714.0883 ± 0.0001 |
| V | 2458716.9608 ± 0.0001 | 2458717.1116 ± 0.0001 |
| R | 2458702.1472 ± 0.0001 | 2458701.9957 ± 0.0001 |
| R | 2458710.9144 ± 0.0001 | 2458711.0653 ± 0.0001 |
| R | 2458713.9377 ± 0.0001 | 2458714.0884 ± 0.0001 |
| R | 2459060.9990 ± 0.0004 | |

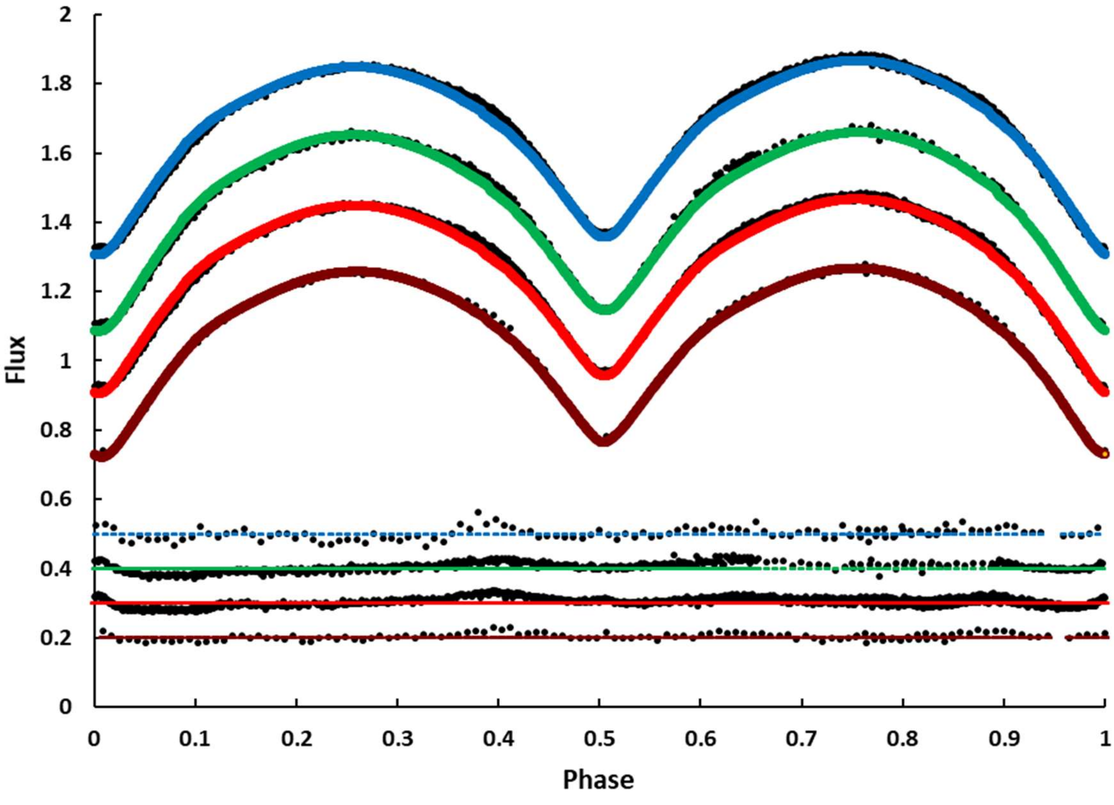


**Figure 2. Observed light curves of BF Pav (points) and modeled solutions (lines) in the BVRI filter from top to bottom, respectively, and residuals are plotted; with respect to orbital phase, shifted arbitrarily in the relative flux.**

## Orbital Period Variations

Using 46 mid-eclipse times including 23 primary and 23 secondary eclipses from the previous study and our observations, we analyze the orbital period variation of this system. All times of minimum listed in Table 3. It includes errors, method or filters of any observation, epochs, O-C values and the references of mid-eclipse times in the last column. We used the linear ephemeris of Gonzalez et al. (1996) for computing epochs and the O-C values.

$$\text{Min. 1 } (BJD_{TDB}) = 2448056.90136\ (0.00020) + 0.30231864\ (0.00000007) \times E \qquad (1)$$

**Table 3. Available times of minima for BF Pav.**

| $BJD_{TDB}$ | Error | Method | Epoch | O-C | References |
|---|---|---|---|---|---|
| 2444438.7617 | | Photoelectric | -11968 | 0.00978 | GCVS 4[3] |
| 2445886.4094 | 0.0001 | Photometer | -7179.5 | 0.00477 | IBVS 3265 |
| 2445886.5621 | 0.0003 | Photometer | -7179 | 0.00631 | IBVS 3265 |
| 2446936.8128 | | CCD | -3705 | 0.00206 | PASP 108 |
| 2446936.8130 | | CCD | -3705 | 0.00226 | PASP 108 |
| 2447259.8384 | | CCD | -2636.5 | 0.00019 | PASP 108 |
| 2447259.8390 | | CCD | -2636.5 | 0.00079 | PASP 108 |
| 2447259.8391 | | CCD | -2636.5 | 0.00089 | PASP 108 |
| 2447368.6720 | | CCD | -2276.5 | -0.00091 | PASP 108 |
| 2447368.6721 | | CCD | -2276.5 | -0.00081 | PASP 108 |
| 2447368.6723 | | CCD | -2276.5 | -0.00061 | PASP 108 |
| 2448056.7487 | | CCD | -0.5 | -0.00144 | PASP 108 |
| 2448056.9008 | | CCD | 0.0 | -0.00050 | PASP 108 |
| 2448056.9013 | 0.0002 | CCD | 0.0 | 0.0 | PASP 108 |
| 2448057.8074 | | CCD | 3 | -0.00085 | PASP 108 |
| 2448057.8075 | | CCD | 3 | -0.00075 | PASP 108 |
| 2448058.8656 | | CCD | 6.5 | -0.00077 | PASP 108 |
| 2448058.8662 | | CCD | 6.5 | -0.00017 | PASP 108 |
| 2449182.7358 | | CCD | 3724 | -0.00021 | PASP 108 |
| 2449182.7361 | | CCD | 3724 | 0.00008 | PASP 108 |
| 2449184.7010 | | CCD | 3730.5 | -0.00008 | PASP 108 |
| 2449184.7007 | | CCD | 3730.5 | -0.00038 | PASP 108 |
| 2449217.5030 | | CCD | 3839 | 0.00034 | PASP 108 |
| 2449217.5031 | | CCD | 3839 | 0.00044 | PASP 108 |
| 2449217.6545 | | CCD | 3839.5 | 0.00068 | PASP 108 |
| 2449217.6550 | | CCD | 3839.5 | 0.00118 | PASP 108 |
| 2449218.5619 | | CCD | 3842.5 | 0.00112 | PASP 108 |
| 2449218.5611 | | CCD | 3842.5 | 0.00032 | PASP 108 |
| 2449219.6189 | | CCD | 3846 | 0.00001 | PASP 108 |
| 2449219.6191 | | CCD | 3846 | 0.00021 | PASP 108 |
| 2457172.7180 | | CCD | 30153 | 0.00265 | OEJV 0179 |
| 2458701.9957 | 0.0001 | CCD | 35211.5 | 0.00151 | This study |
| 2458702.1472 | 0.0001 | CCD | 35212 | 0.00195 | This study |
| 2458710.9144 | 0.0001 | CCD | 35241 | 0.00191 | This study |
| 2458711.0653 | 0.0001 | CCD | 35241.5 | 0.00165 | This study |
| 2458713.9377 | 0.0001 | CCD | 35251 | 0.00192 | This study |
| 2458713.9377 | 0.0001 | CCD | 35251 | 0.00192 | This study |
| 2458713.9377 | 0.0001 | CCD | 35251 | 0.00202 | This study |
| 2458713.9380 | 0.0002 | CCD | 35251 | 0.00232 | This study |
| 2458714.0882 | 0.0001 | CCD | 35251.5 | 0.00136 | This study |

[3]http://www.sai.msu.su/gcvs/gcvs/

| | | | | | |
|---|---|---|---|---|---|
| 2458714.0883 | 0.0001 | CCD | 35251.5 | 0.00146 | This study |
| 2458714.0883 | 0.0002 | CCD | 35251.5 | 0.00146 | This study |
| 2458714.0884 | 0.0001 | CCD | 35251.5 | 0.00156 | This study |
| 2458716.9608 | 0.0001 | CCD | 35261 | 0.00193 | This study |
| 2458717.1116 | 0.0001 | CCD | 35261.5 | 0.00157 | This study |
| 2459060.9990 | 0.0004 | CCD | 36399 | 0.00152 | This study |

A new linear ephemeris was determined by fitting a line to mid-eclipse times using the least-squares method,

$$\text{Min. 1 (BJD}_{\text{TDB}}) = (2448056.90288 \pm 0.00236) + (0.302318644 \pm 0.000000073) \times E\ days \qquad (2)$$

where E is the cycle number after the reference cycle. Figure 3 shows the O-C diagram calculated using Equation 2 and all times of minimum listed in Table 3. Where no error estimate was reported in the original references, we assumed a value equal to the largest reported error. The solid black line represents a quadratic least squares fit to the O-C values. The quadratic ephemeris is given in Equation 3,

$$\text{Min. 1 (BJD}_{\text{TDB}}) = (2448056.90197 \pm 0.00006) + (0.302318221 \pm 0.000000012) \times E + (1.277436015 \pm 0.037588002) \times 10^{-11} E^2\ days. \qquad (3)$$

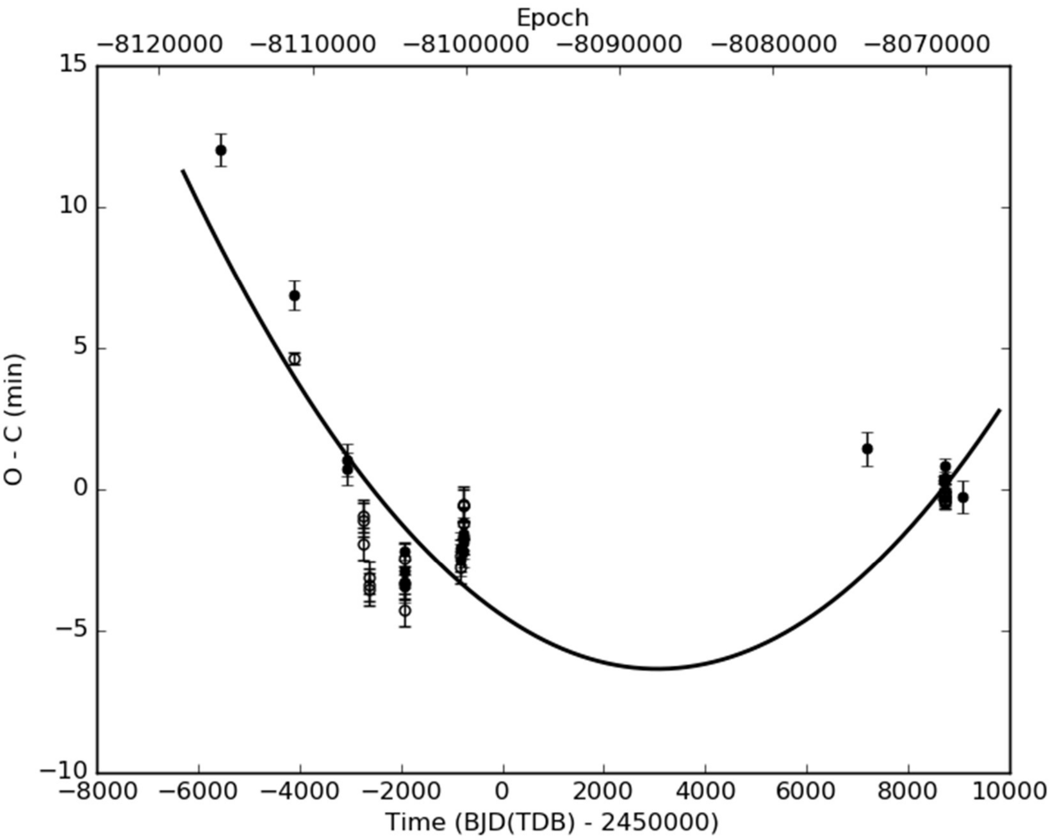


**Figure 3. The quadratic trend on the data points in residual of the linear fit.**

We calculate $\dot{p}$, the rate of period change, using following formula according to a small quadratic term in the residue O-C,

$$\frac{dp}{dE} = 2Q \qquad (4)$$

It reveals a continuous period increase at a rate of 0.3086634$\times 10^{-7}$ $day/yr$ which corresponds to a period increase of 0.266 s $century^{-1}$.

The fitted quadratic trend in O-C derived by the Monte Carlo Markov Chain (MCMC) approach in OCFit code[4] with 1000000 MC steps and 20000 burn-in steps. Confidence interval plots for fitted parameters of $p. t_0. and\ Q$; and distributions of these parameters determined by the MCMC approach are displayed in Figure 4 and Figure 5, respectively.

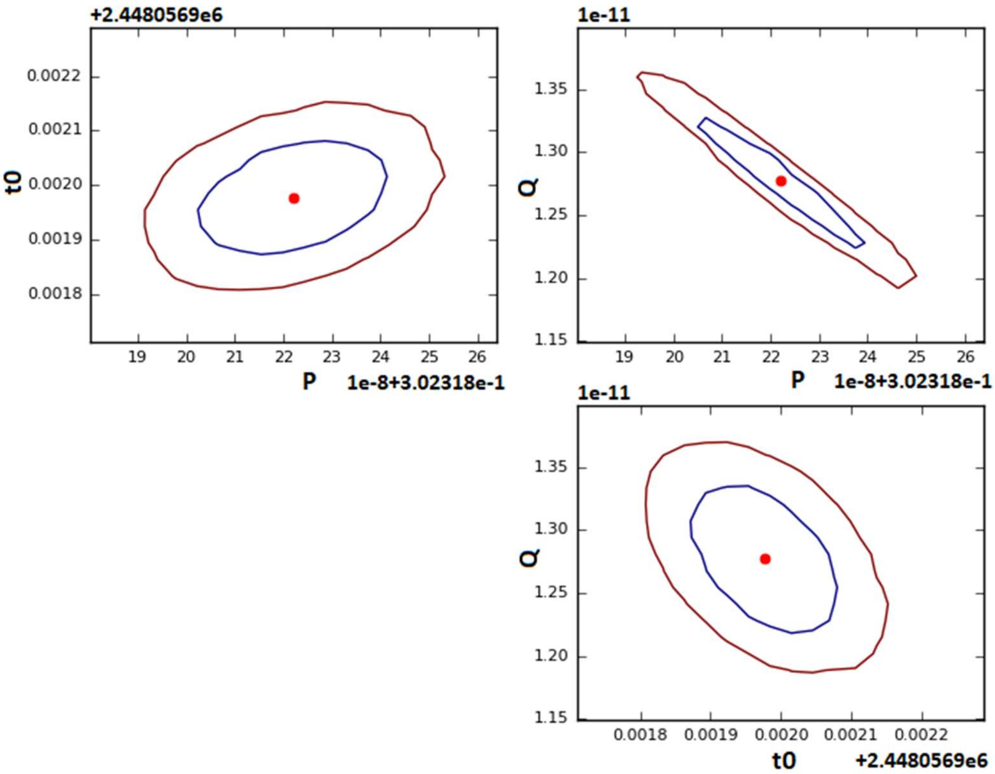


**Figure 4. The plot of Confidence Regions for 1$\sigma$=0.6827 and 2$\sigma$= 0.9545 induced via the MCMC approach.**

[4]https://github.com/pavolgaj/OCFit

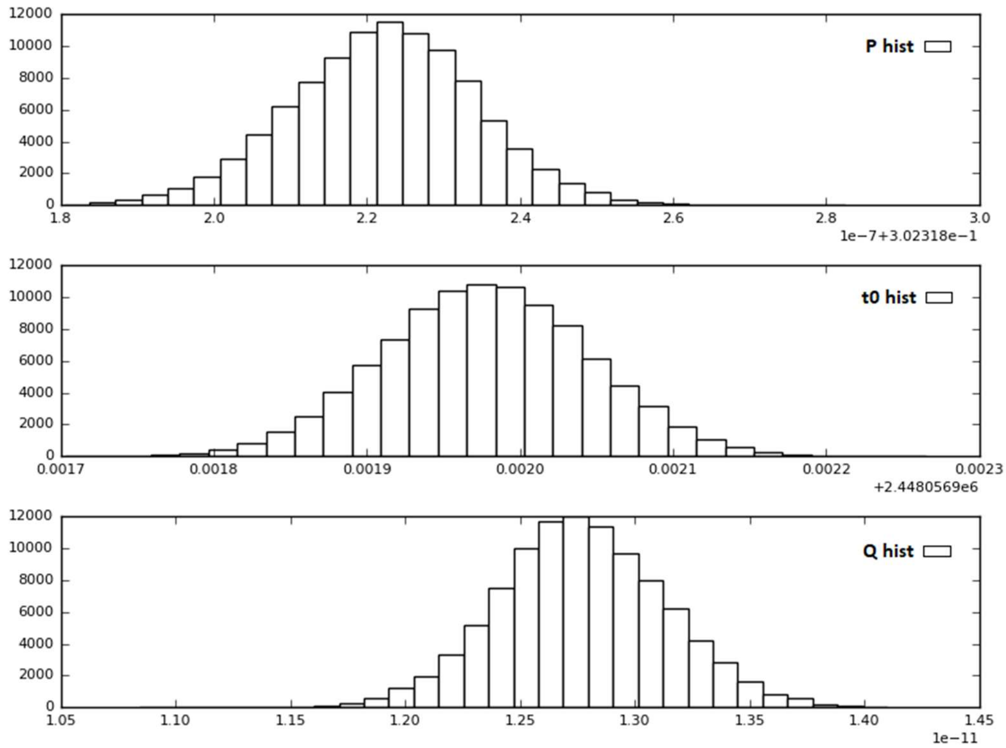


**Figure 5. Distribution of parameters of P, $t_0$, and Q (from up to down respectively) induced by the MCMC approach.**

In Figure 6, a cyclic change is clearly seen in the residual of the quadratic term. Therefore, BF Pav is a good choice for more photometric and spectroscopic observations in the future.

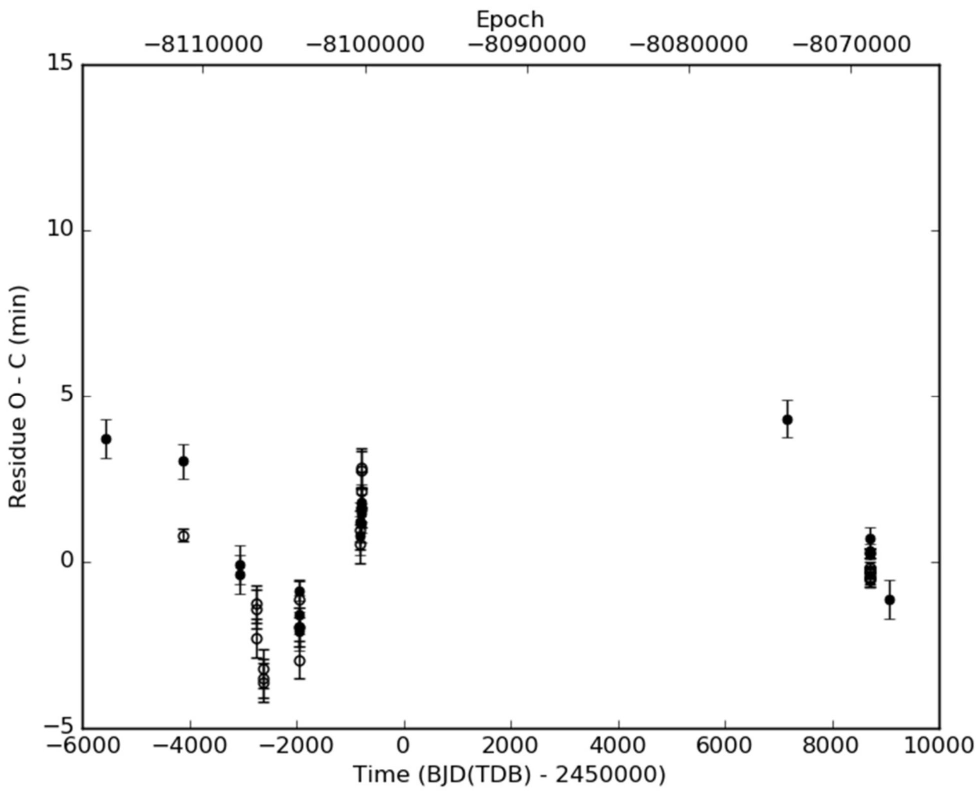


**Figure 6. A cyclic trend is seen in the residual of the quadratic trend of O-C.**

## Light curve analysis

We used PHOEBE (PHysics Of Eclipsing BinariEs) legacy 0.32 version, based on the Wilson-Devinney code (Prša and Zwitter, 2005), to analyze the light curves.

The mass ratio of the system could obtain by the q-search method in the photometric observations, so we did it according to the required standards. As can be seen in Figure 7, there is a deep minimum in the q-search of BF Pav. Accordingly, in the range of fixed mass ratios from 0.1 to 1.3, a minimum value of $\sum(O-C)^2$ was initially achieved at $q$ = 0.94.

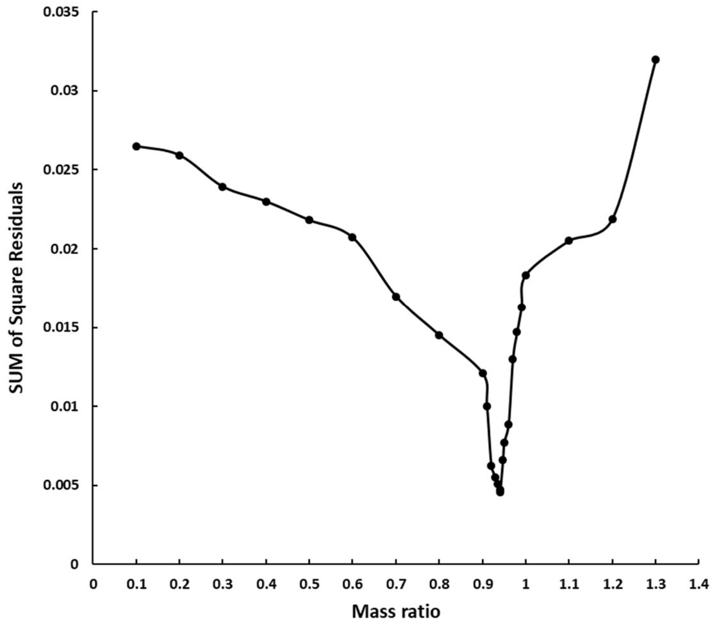


**Figure 7. Sum of the squared residuals as a function of the mass ratio.**

The (B-V) color index is the difference in magnitudes between two wavelength filters B and V. The blue and visual magnitudes that they are measured through filters centered at 442 nm and 540 nm, respectively. Passing light through different filters depends on the star's surface temperature according to the Planck Law radiation distributions. It means that by having data of the Blue and Visual filters we can calculate the (B-V) index and obtain a good estimation of a star's surface temperature by it (Poro et al., 2020).

The fraction of detected flux of wavelength depends on the telescope mirrors, the bandwidth of filters, and the response of the photometer, thus it is necessary to correct our data by calibration with the comparison star from standard catalogs.

Many studies presented relations between the (B-V) index and the surface temperature of the star such as Code et al. (1976), Sekiguchi and Fukugita (2000), and Ballesteros (2012). Eker et al. (2018) presented relations and tables for different parameters of the main-sequence stars. Eker et al. (2018) selected absolute parameters of 509 main-sequence stars from the components of detached-eclipsing spectroscopic binaries in the solar neighborhood that are used to study Mass-Luminosity, Mass-Radius, and Mass-Temperature relations. They combined the photometric data of Sejong Open cluster Survey (SOS) and typical absolute parameters adjusted from the MLR, MRR, and MTR functions calibrated in their study. 'Sejong Open cluster Survey (SOS) is a photometry project of a large number of clusters in the SAAO Johnson-Cousins' UBVI system by Sung et al. (2013).

Based on our data and after calibrating (Høg et al., 2000), we calculated $(B-V)_{BF\ Pav} = 0^m.803$. As a result, based on Eker et al. (2018), the effective temperature of the primary component found to be 5201 K.

Sekiguchi and Fukugita (2000) derived a (B-V) color-temperature relation too. They present $T_{eff}$ as a function of (B-V) color index to represent the metallicity value in four classes. By combining the previous results from Eker et al. (2018) and exerting the results of Sekiguchi and Fukugita (2000), the metallicity value for the primary component of BF Pav can be estimated between -0.75 and -0.25 (star's population II). As shown in Figure 8, obtained temperature from derived (B-V) color is also in an acceptable range (4800 K - 5300 K) for the primary component of BF Pav with the method of Sekiguchi and Fukugita (2000).

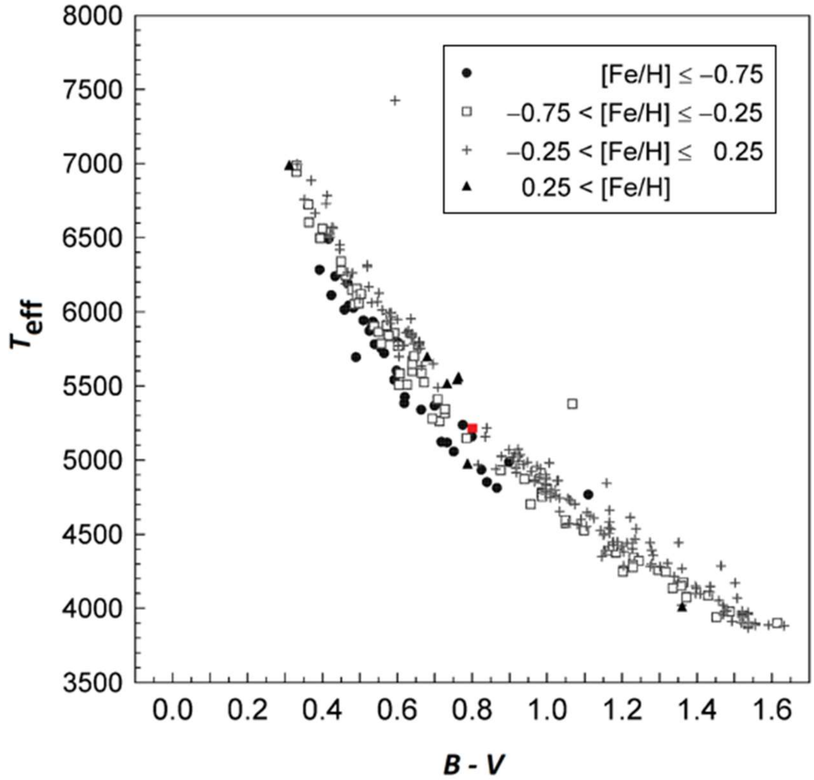


**Figure 8. BF Pav's position (red dot) based on the Sekiguchi and Fukugita (2000) results.**

We assumed gravity-darkening coefficients $g_1 = g_2 = 0.32$ (Lucy, 1967), bolometric albedo $A_1 = A_2 = 0.5$ (Rucinski, 1969), and linear limb darkening coefficients taken from tables published by Van Hamme (1993).
As can be inferred from the light curves, the mean minimum occurred first, and also the temperature of the primary star is higher than the secondary. Based on the unequal minimums, and the logical light curve solutions, mode 3 was chosen for analysis. The parameters obtained from the solutions are given in Table 4.
The mean fractional radii of components were calculated with the formula, $r_{mean} = (r_{back} \times r_{side} \times r_{pole})^{1/3}$.

**Table 4. Photometric solutions of BF Pav.**

| Parameter | Results |
|---|---|
| $T_1$ (K) | 5201(13) |
| $T_2$ (K) | 5050(21) |
| $\Omega_1=\Omega_2$ | 3.584(24) |
| i (deg) | 86.747(45) |
| $q=m_2/m_1$ | 0.94(4) |
| $l_1/l_{tot}$(V) | 0.550(6) |
| $l_2/l_{tot}$(V) | 0.449 |
| $l_1/l_{tot}$(B) | 0.532(5) |
| $l_2/l_{tot}$(B) | 0.468 |
| $l_1/l_{tot}$(R) | 0.540(5) |
| $l_2/l_{tot}$(R) | 0.459 |
| $l_1/l_{tot}$(I) | 0.483(7) |

| | |
|---|---|
| $l_2/l_{tot}(I)$ | 0.516 |
| $A_1=A_2$ | 0.50 |
| $g_1=g_2$ | 0.32 |
| $f$ (%) | 13 |
| $r_1$(back) | 0.425 |
| $r_1$(side) | 0.390 |
| $r_1$(pole) | 0.370 |
| $r_2$(back) | 0.415 |
| $r_2$(side) | 0.379 |
| $r_2$(pole) | 0.359 |
| $r_1$(mean) | 0.394(16) |
| $r_2$(mean) | 0.383(15) |
| $Colatitude_{spot}$ (deg) | 67 |
| $Longitude_{spot}$ (deg) | 112(8) |
| $Radius_{spot}$ (deg) | 16(9) |
| $T_{spot}/T_{star}$ | 0.96(4) |
| $\sum(O-C)^2$ | 0.004 |
| Phase Shift | 0.004(1) |

Note: Parameters of a star spot is on the primary component.

A difference in the heights of the maxima in light curves of eclipsing binary systems indicates the O'Connell effect (O'Connell, 1951). This binary system appears to demonstrate this effect because we need to add a spot on the primary component in the light curve solutions. Table 5 represents the characteristic parameters of the light curves of BF Pav.

**Table 5. Characteristic parameters of the light curves in the BVRI filters.**

| Part of LC. | B | V | R | I |
|---|---|---|---|---|
| MaxI - MaxII | 0.032 | 0.005 | 0.027 | 0.011 |
| MaxI - MinI | -1.052 | -0.982 | -0.920 | -0.879 |
| MaxI - MinII | -0.868 | -0.820 | -0.783 | -0.780 |
| MinI - MinII | 0.184 | 0.162 | 0.137 | 0.099 |

Fillout factor is a quantity that indicates the degree of contact in the binary star systems defined by Mochnacki & Doughty (1972) and Lucy & Wilson (1979) that was modified and redefined by David H. Bradstreet (2005),

$$f = \frac{\Omega(L_1) - \Omega}{\Omega(L_1) - \Omega(L_2)} \qquad (5)$$

where $\Omega.\Omega(L_1)$ ,and $\Omega(L_2)$ are star surface potential, inner Lagrangian surface potential, and outer Lagrangian surface potential, respectively. We calculated a fillout factor of 13% from the output parameters of the light curve solutions.

The $M_{(primary)}$ is derived from a study by Eker et al. (2018), and $M_{(secondary)}$ is calculated by $q = \frac{M_2}{M_1}$. We also calculated the mass of each component of the binary system using the method of Harmanec (1988) who derived a simple approximation formula relating absolute parameters (mass, radius and luminosity) to the effective temperature of the components based on data analyzing. For this purpose, we used the following formula,

$$logM/M_{\odot} = ((1.771141X - 21.46965)X + 88.05700)X - 121.6782) \qquad (6)$$

where X is $\log(T_{eff})$. This formula is only defined in the range of $4.62 \geq \log(T_{eff}) \geq 3.71$ (Harmanec, 1988). As the mentioned range is valid for BF Pav due to our photometric solution, we calculated $M_1$ and $M_2$. The absolute parameters are given in the Table 6 and there is a high conformity between the results which were obtained by two methods.

**Table 6. Estimated absolute parameters of BF Pav by two methods to calculate the mass of the primary component.**

| | Eker et al. (2018) | | Harmanec (1988) | |
|---|---|---|---|---|
| **Parameter** | **Primary** | **Secondary** | **Primary** | **Secondary** |
| Mass ($M_\odot$) | 0.914 | 0.859(20) | 0.906(18) | 0.857(18) |
| Radius ($R_\odot$) | 0.904(56) | 0.878(53) | 0.902(56) | 0.876(54) |
| Luminosity ($L_\odot$) | 0.536(72) | 0.450(62) | 0.534(61) | 0.448(69) |
| $M_{bol}$ (mag) | 5.42(15) | 5.61(15) | 5.42(15) | 5.61(15) |
| log g (cgs) | 4.486(44) | 4.485(42) | 4.484(44) | 4.486(42) |
| a ($R_\odot$) | 2.294(5) | | 2.289(5) | |

According to the estimated absolute parameters of this binary system, the distance was calculated. We obtained $m_v$ = 12.674(25) from our light curve and $M_v$ = 5.601(30) for primary component ($BC_1$ = -0.181 from Eker et. al., 2018). So the distance to the binary system compute from the equation,

$$d_{(pc)} = 10^{\left(\frac{m_{pri}-M_{pri}+5-A_V}{5}\right)} \qquad (7)$$

Therefore, an estimate of the distance of this binary system is 250 ± 27 parsec (using with $A_v$ = 0.08 (Schlafly and Finkbeiner, 2011).

The 3D view of BF Pav and the Roche lobe configuration of BF Pav is illustrated in Figure 9.

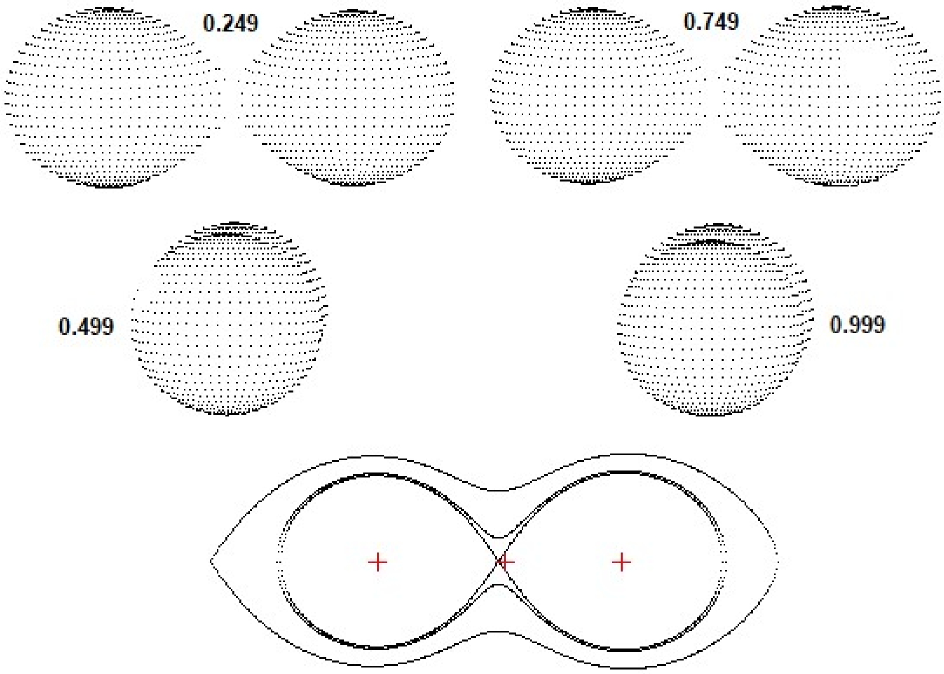


**Figure 9. The positions of the components of BF Pav.**

## Results and Conclusion

This study's approach is to present a new ephemeris and light curve analysis of the W UMa-type eclipsing binary, BF Pav and probe this binary system's period changes. The photometric observations of BF Pav were carried out during five nights utilizing BVRI filters. We specified the photometric solution of the short period binary BF Pav based on the Wilson-Devinney code through the analysis of the light curves. Our results suggest that BF Pav is a contact binary with a mass ratio ($q = \frac{M_2}{M_1}$) of 0.94 from q-search, and a fillout factor (*f*) of 13%, and the difference between this binary system components' temperature ($\Delta T$) of 151 K. Also, we calculated the binary system distance which is equal to 250 ± 27 pc and this result is in good agreement with the Gaia DR2[5] value 255.084 ± 2.770 pc. We calculated the mass of each component of the binary system from two methods and their value were close to each other.

Based on the estimation of absolute parameters, the diagrams of the Mass-Luminosity (M-L) and the Mass-Radius (M-R) on a log-scale (Figure 10) show the evolutionary status of BF Pav. The theoretical ZAMS and TAMS lines and the positions of the primary and secondary components are depicted in the diagrams.

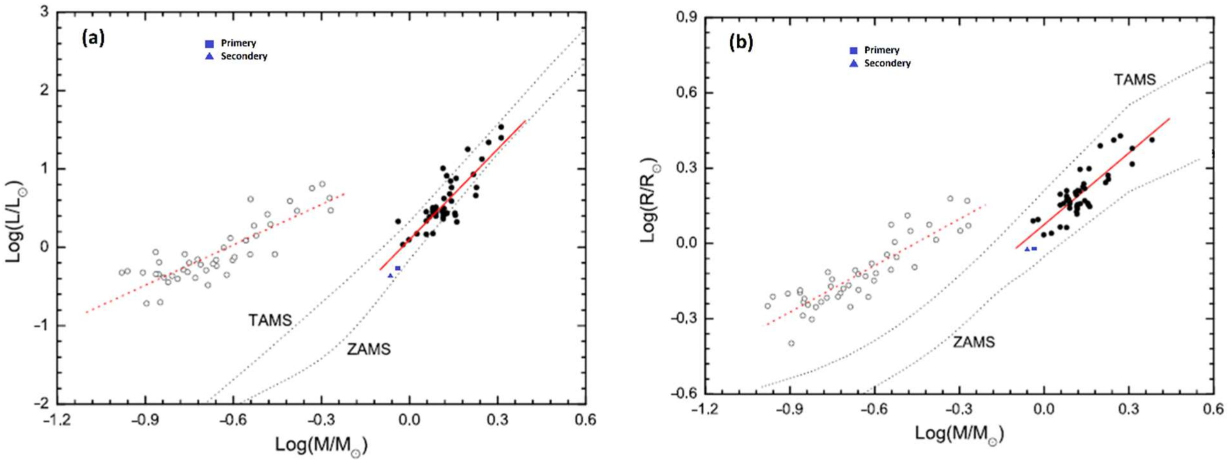


**Figure 10. The log M - log L, and log M - log R diagrams for BF Pav from the absolute parameters.**

Stellar winds are the major responsible for the binary system's mass loss due to the star's magnetic activities. According to the Table 5 and maxima differences in the light curves, it seems that BF Pav does not have significant magnetic activity and this implies a negligible O'Connell effect in this binary system, we fetched up that the mass loss idea is void for this binary system, so we concentrate on mass transfer. Based on the third Kepler law ($p^2 = \frac{4\pi^2}{G(M_1+M_2)} a^3$ (7)), by considering the angular momentum conservation law, we used the following formula (Negu and Tessema, 2015):

$$\frac{\dot{p}}{p} = 3\dot{M}_1 \frac{(M_1 - M_2)}{M_1 M_2} \qquad (8)$$

According to our results, the primary star mass is more than secondary star mass ($M_1 > M_2$) and also $\dot{p} > 0$ from our O-C analysis, so we derive that $\dot{M}_1 > 0$, thus the mass transfer is from the less massive star to the more massive star, from the secondary star to the primary star, which causes $\dot{a} > 0$ ($\frac{\dot{p}}{p} = \frac{3}{2}\frac{\dot{a}}{a}$) that means the orbit enlarges and the angular frequency ($\frac{\dot{\omega}}{\omega} = \frac{-\dot{p}}{p}$) decreases.

BF Pav had been observed by Hoffman (1981) but the observer has not been able to prosecute a detailed analysis due to lack of data. After a while, the first detailed photometric analysis of BF Pav was performed in 1996 using the Wilson-Devinney code (Gonzalez et al., 1996) after UBV photoelectric observations of this binary system

[5] https://www.cosmos.esa.int/web/gaia/dr2

between 1987 and 1993 in the observational program of southern short-period eclipsing binaries. The former photometric solution demonstrates that BF Pav has a mass ratio of 1.4 ($M_1 < M_2$) while we calculated the amount of q by two methods, one from light curve solutions and one from Hermance (1988) method, and the result of both of them are very close to each other and the value of them is 0.94 ($M_1 > M_2$) up to two decimal digits. To complete our comparison, we found 13% for the amount of fillout factor whereas 10% was obtained for $f$ in the prior study. The temperature of the primary star reported 5430 K in the first photometric solution whereas we found 5201 K and concerning the upper temperature limit value for this binary system's primary star is 5200 K in Gaia DR2, the previously reported amount for the primary effective temperature is not located in the admissible range.

**Acknowledgments**
This manuscript is based on the Binary Systems of South and North (BSN) project. The project aims to study contact binary systems in the northern and southern hemispheres of several observatories in different countries.

## References

[1] Ballesteros, F.J., 2012. New insights into black bodies. *EPL (Europhysics Letters)*, *97*(3), p.34008.
[2] Bradstreet, D.H., 2005, May. Fundamentals of solving eclipsing binary light curves using Binary Maker 3. In *Society for Astronomical Sciences Annual Symposium* (Vol. 24, p. 23).
[3] Code, A.D., Bless, R.C., Davis, J. and Brown, R.H., 1976. Empirical effective temperatures and bolometric corrections for early-type stars. *The Astrophysical Journal*, *203*, pp.417-434.
[4] Collins, K.A., Kielkopf, J.F., Stassun, K.G. and Hessman, F.V., 2017. AstroImageJ: Image processing and photometric extraction for ultra-precise astronomical light curves. *The Astronomical Journal*, *153*(2), p.77.
[5] Davoudi, F., Jafarzadeh, S.J., Poro, A., Basturk, O., Mesforoush, S., Harandi, A.F., Gozarandi, M.J., Mehrjardi, Z.Z., Maley, P.D., Khakpash, S. and Rokni, K., 2020. Light curve analysis of ground-based data from exoplanets transit database. *New Astronomy*, *76*, p.101305.
[6] Dryomova, G.N. and Svechnikov, M.A., 2006. Variation in the orbital period of W UMa-type contact systems. *Astrophysics*, *49*(3), pp.358-369.
[7] Eker, Z., Bakış, V., Bilir, S., Soydugan, F., Steer, I., Soydugan, E., Bakış, H., Aliçavuş, F., Aslan, G. and Alpsoy, M., 2018. Interrelated main-sequence mass–luminosity, mass–radius, and mass–effective temperature relations. *Monthly Notices of the Royal Astronomical Society*, *479*(4), pp.5491-5511.
[8] Gonzalez, J.F., Lapasset, E., Gomez, M. and Ahumada, J., 1996. Photometric Analysis of the Contact Binary BF Pavonis. *Publications of the Astronomical Society of the Pacific*, *108*(722), p.338.
[9] Harmanec, P., 1988. Stellar masses and radii based on modern binary data. *Bulletin of the Astronomical Institutes of Czechoslovakia*, *39*, pp.329-345.
[10] Hoffmann, M., 1981. Photoelectric Photometry of BF Pavonis. *Information Bulletin on Variable Stars*, *1935*.
[11] Høg, E., Fabricius, C., Makarov, V.V., Bastian, U., Schwekendiek, P., Wicenec, A., Urban, S., Corbin, T. and Wycoff, G., 2000. Construction and verification of the Tycho-2 Catalogue. Astronomy and Astrophysics, 357, pp.367-386.
[12] Juryšek, J., Hoňková, K., Šmelcer, L., Mašek, M., Lehký, M., Bílek, F., Mazanec, J., Hanžl, D., Magris, M., Nosál, P. and Bragagnolo, U., 2017. BRNO Contributions# 40 Times of minima. *OEJV*, *179*, p.1.
[13] Kwee, K. and Van Woerden, H., 1956. A method for computing accurately the epoch of minimum of an eclipsing variable. *Bulletin of the Astronomical Institutes of the Netherlands*, *12*, p.327.
[14] Lucy, L.B., 1967. Gravity-darkening for stars with convective envelopes. *Zeitschrift fur Astrophysik*, *65*, p.89.
[15] Lucy, L.B. and Wilson, R.E., 1979. Observational tests of theories of contact binaries. *The Astrophysical Journal*, *231*, pp.502-513.
[16] Mochnacki, S.W. and Doughty, N.A., 1972. A Model for the Totally Eclipsing W Ursae Majoris System AW UMa. *Monthly Notices of the Royal Astronomical Society*, *156*(1), pp.51-65.
[17] Negu, S.H. and Tessema, S.B., 2015. Mass Transfer in Binary Stellar Evolution and Its Stability. *International Journal of Astronomy and Astrophysics*, *5*(03), p.222.

[18] O'Connell, D.J.K., 1951. The so-called periastron effect in eclipsing binaries. *Monthly Notices of the Royal Astronomical Society*, *111*(6), pp.642-642.
[19] Poro, A., Davoudi, F., Basturk, O., Esmer, E.M., Aksaker, N., Akyüz, A., Aladağ, Y., Rahimi, J., Lashgari, E., Ghanbarzadehchaleshtori, M. and Modarres, S., 2020. The First Light Curve Solutions and Period Study of BQ Ari. *arXiv preprint arXiv:2006.00528*.
[20] Prša, A. and Zwitter, T., 2005. A computational guide to physics of eclipsing binaries. I. Demonstrations and perspectives. *The Astrophysical Journal*, *628*(1), p.426.
[21] Rucinski, S.M., 1969. The proximity effects in close binary systems. II. The bolometric reflection effect for stars with deep convective envelopes. *Acta Astronomica*, *19*, p.245.
[22] Schlafly, E.F. and Finkbeiner, D.P., 2011. Measuring reddening with Sloan Digital Sky Survey stellar spectra and recalibrating SFD. *The Astrophysical Journal*, *737*(2), p.103.
[23] Sekiguchi, M. and Fukugita, M., 2000. A Study of the B− V Color-Temperature Relation. *The Astronomical Journal*, *120*(2), p.1072.
[24] Smith, R.C., 1984. The theory of contact binaries. *Quarterly Journal of the Royal Astronomical Society*, *25*(4), pp.405-420.
[25] Spencer Jones, J.H., 1988. The W UMa Stars AB Tel and BF Pav. *IBVS*, *3265*, p.1.
[26] Sung, H., Lim, B., Bessell, M.S., Kim, J.S., Hur, H., Chun, M.Y. and Park, B.G., 2013. Sejong open cluster survey (SOS). 0. Target selection and data analysis. *arXiv preprint arXiv:1306.0309*.
[27] Van Hamme, W., 1993. New limb-darkening coefficients for modeling binary star light curves. *The Astronomical Journal*, *106*, pp.2096-2117.
[28] Zhang, L., Pi, Q., Han, X.L., Li, T., Zhang, X., Sang, H., Wang, D. and Wang, S., 2015. The first multi-color photometric study of the short-period contact eclipsing binary GK Aqr. *New Astronomy*, *38*, pp.50-54.